Altered exosomal microRNA profiles in bronchoalveolar lavage fluid can mediate metabolism in patients with *Acinetobacter baumannii* ventilator-associated pneumonia

Bo Zhou[1#], Manyun Guo[2], Xiang Hao[2], Bowen Lou[2], Junhui Liu[3#], Jianqing She[2#]

[1]Respiratory and Critical Care Medicine, the First Affiliated Hospital of Xi'an Jiaotong University, Xi'an, China; [2]Cardiovascular Department, the First Affiliated Hospital of Xi'an Jiaotong University, Xi'an, China; [3]Diagnostic Department, the First Affiliated Hospital of Xi'an Jiaotong University, Xi'an, China

Contributions: (I) Conception and design: B Zhou, J Liu, J She; (II) Administrative support: B Zhou, J Liu, J She; (III) Provision of study materials or patients: B Zhou, M Guo, B Lou; (IV) Collection and assembly of data: B Zhou, X Hao, B Lou; (V) Data analysis and interpretation: M Guo, X Hao, B Lou; (VI) Manuscript writing: All authors; (VII) Final approval of manuscript: All authors.

[#]These authors contributed equally to this work as co-first authors.

Correspondence to: Jianqing She. Cardiovascular Department, the First Affiliated Hospital of Xi'an Jiaotong University, Xi'an, China. Email: jianqingshe@xjtu.edu.cn; Junhui Liu. Diagnostic Department, the First Affiliated Hospital of Xi'an Jiaotong University, Xi'an, China. Email: liu1109@xjtu.edu.cn; Bo Zhou. Respiratory and Critical Care Medicine, the First Affiliated Hospital of Xi'an Jiaotong University, Xi'an, China. Email: zb_bob@stu.xjtu.edu.cn.

Background: Ventilator-associated pneumonia (VAP) is a major public health problem and is most commonly caused by *Acinetobacter baumannii* (Ab) infection. In our study, we investigated the profiles of exosomal microRNAs (miRNAs) extracted from the bronchoalveolar lavage fluid (BALF) and serum of patients with *Acinetobacter baumannii* ventilator-associated pneumonia (Ab-VAP). We also examined the serum metabolomic profiles of these patients. Our aim was to study the associations between lung tissue-derived exosomal miRNAs and changes in global metabolism in patients with Ab-VAP.

Methods: Consecutively sampled patients admitted to an intensive care unit (ICU) for pulmonary infection treatment were enrolled in this study. Demographic information and biochemical measurements were collected. Serum samples were obtained following overnight fasting on admission. Bronchoscopies were performed and BALF samples were collected from each patient. Exosomes were extracted using kits from System Biosciences (SBI) and miRNA sequencing was performed. Non-targeted metabolomics were used to express metabolic profiles.

Results: We found significant changes in the miRNA profiles of patients with Ab-VAP; these changes occurred in both BALF exosomal miRNA and serum exosomal miRNA. Gene Ontology analysis further identified the function of miRNA in system metabolism. Serum metabolomic profiles and ratios of biological significance were found to be differentially regulated in Ab-VAP patients. This differential regulation was correlated with the differential expression of miRNAs.

Conclusions: Our data summarizes the dysregulation of serum metabolism and exosomal miRNA excretion that occurs in Ab-VAP patients. The correlation found between BALF exosomal miRNA and dysregulated metabolism, as indicated by the irregular expression of metabolites in the cellular metabolic pathway, highlights potential biomarkers for the diagnosis and treatment of Ab infection.

Keywords: *Acinetobacter baumannii*; exosomes; MicroRNA profiles; metabolomics; ventilator-associated pneumonia (VAP)

Submitted Mar 10, 2020. Accepted for publication Sep 11, 2020.

doi: 10.21037/atm-20-2375

View this article at: http://dx.doi.org/10.21037/atm-20-2375

© Annals of Translational Medicine. All rights reserved.

Introduction

Ventilator-associated pneumonia (VAP) is a major public health concern due to the increasing morbidity and mortality rates among intensive care unit (ICU) patients (1). *Acinetobacter baumannii* (Ab) is the most common pathogen known to cause VAP (2). As antimicrobial resistance is prevalent in patients infected with Ab, options for treating this infection are limited (3). Therefore, a better understanding of the pathophysiology of Ab infection is of great clinical significance for the development of targeted novel therapies for patients with *Acinetobacter baumannii* ventilator-associated pneumonia (Ab-VAP).

Previous research that examined bronchoalveolar lavage fluid (BALF) found that "exosome containers" in this fluid mediate intercellular communication in respiratory diseases (4-6). Exosomes have been shown *in vivo* to serve as containers that carry and rapidly release selective molecules, such as microRNAs (miRNAs) and long non-coding RNAs (lncRNAs) (7). Recent studies have also shown that exosomal miRNAs in BALF and serum exhibit distinct features in patients with asthma, acute respiratory distress syndrome, and pulmonary infection (5,8-11). Exosomes transfer miRNAs to target cells, allowing these miRNAs to exert their effects on these targets (12). Patients with pulmonary infection, particularly that caused by Ab, often exhibit systemic inflammasome activation and metabolism dysregulation (1); however, there is a lack of evidence describing the mechanisms by which BALF exosomes modulate these patients' circulatory metabolism and influence disease progression.

Metabolomics studies have shown that alterations occur in the circulatory metabolism of patients with pulmonary infection (13,14). Critical pulmonary infection can cause malnutrition, gut microbiota dysregulation, and changes in energy metabolism, which can result in metabolic disturbance (15-17). Due to its persistent course, the metabolic features of Ab infection are well defined. However, few studies have discussed the global metabolic profiles of patients with Ab-VAP and the mechanisms by which they are dysregulated. Recent studies have shown that adipose-derived exosomal miRNAs can modulate systemic metabolism by interfering with gene expression in distant tissues, providing a novel mechanism of cell–cell crosstalk (7). However, the effect of altered BALF exosomal miRNA profiles on serum metabolite profiles during pulmonary infection has not been explored. We therefore hypothesized that BALF exosomes released from both immune and structural lung cells carry miRNAs to target organs where they exert effects that alter the serum metabolite profiles of Ab-VAP patients.

In this study, we investigated BALF exosomal miRNA profiles and serum metabolic profiles to study the associations between lung tissue-derived exosomal miRNAs and changes in the global metabolism of Ab-VAP patients. We showed that the profile of exosomal miRNAs expressed in BALF and serum, as well as the serum metabolite profiles, were significantly different in Ab-VAP patients compared with community-acquired pneumonia (CAP) patients. These altered exosomal miRNA profiles were significantly enriched in cellular metabolic pathways and notably correlated with the metabolism of alcohols, indoles, and alkylamines. This study provides new evidence that highlights how lung tissue-derived exosomal miRNAs affect systemic metabolism. We also revealed potential therapeutic targets for the treatment of Ab infection.

Methods

Subjects

Between March 2018 and September 2018, 40 patients that attended the First Affiliated Hospital of Xi'an Jiaotong University in China were enrolled in this study. Of these patients, 15 were diagnosed with VAP and 25 were diagnosed with CAP; the CAP patients were the control group. The age range of the study cohort was 50–75 years. This study was approved by the Ethics Committee of Xi'an Jiaotong University (2018G-169), and all patients gave written informed consent according to the Declaration of Helsinki (as revised in 2013). Ab was present in the BALF collected from VAP patients; it was not present in that of CAP patients. Subjects were excluded if they met any of the following criteria: they were taking or had previously taken any drugs known to influence lipid metabolism or endocrine function; they had a chronic respiratory disease, cardiac disease, or endocrine disease; they were undergoing hemodialysis for renal failure; they had acute or chronic hepatitis with increased transaminase activities; or they had a malignant tumor. Demographic information and biochemical measurements were obtained from all subjects as described in previous studies (18-20).

BALF and serum collection and isolation of exosomes

During bronchoscopy, 20 mL of BALF was collected

© Annals of Translational Medicine. All rights reserved.

from each patient. Serum from participants was collected after overnight fast. The collected BALF and serum were then centrifuged at 3,000 rpm for 15 min to separate cells and cell debris. The supernatant was then removed. Following the manufacturer's instructions, exosomes were precipitated using System Biosciences' (SBI's) ExoQuick Kit. The precipitated exosomes were then resuspended in 100 µL 1× phosphate-buffered saline (PBS). The size and morphology of the exosomes were examined using a Hitachi HT7700 electron microscope (21). Each preparation of exosomes was based on Minimal Information for Study of Extracellular Vesicles 2018 (MISEV2018), including quantitative measures of BALF exosomes, testing for exosome abundance (protein content), and the presence of exosome-associated components. The protein concentrations of the resuspended pellet preparations were measured by detergent compatible (DC) protein assay (Bio-Rad Laboratories, Hercules, CA, USA) according to the manufacturer's instructions.

Exosomal miRNA sequencing

Trizol reagent (1 mL) was added to the exosome suspension, and RNA was extracted following the Trizol reagent manual. The RNA was precipitated in 1:1 isopropanol (v/v) and 1 µL glycogen at –20 ℃ overnight. An exosomal miRNA library was constructed with a QIAseq miRNA library construction kit (QIAGEN) used in accordance with the manufacturer's instructions. Libraries were sequenced on an Illumina HiSeq-2500 sequencer for 50 cycles. Reads that passed the Illumina quality filters were retained for analysis. Adapters were trimmed from the reads and reads shorter than 17 nt were discarded. The remaining reads were then mapped to the miRBase human miRNA reference database using the FANSe3 algorithm on the Chi-Cloud NGS Analysis Platform (Chi-Biotech Co. Ltd., Shenzhen, China) (21).

Serum sample preparation and biochemical measurements

Serum samples were collected from both VAP and CAP patients on admission. Fasting venous blood was withdrawn the next morning and immediately centrifuged at 3,000 rpm for 10 min at 4 ℃. Separated serum was stored at –80 ℃ and aliquots were thawed for later processing as described in previous publications (18,20). Biochemical tests, including a complete blood count, a c-reactive protein (CRP) test, a procalcitonin (PCT) test, and tests for liver and kidney function, were administered following blood collection to determine if subjects should be included or excluded in the study.

Serum metabolism profile determination

Non-targeted metabolomics profiling was performed using the XploreMET platform (Metabo-Profile Biotechnology, Shanghai, China) (18,20). The sample preparation, instrumentation, metabolic annotation, and data analysis procedures were carried out as described in previous publications (22-24) with some minor modifications. The metabolites detected by this process included alcohols, aldehydes, alkylamines, amino acids, carbohydrates, fatty acids, hormones, indoles, lipids, nucleotides, organic acids, phenols, and vitamins. The ratios between metabolites correlated with biological significance were also calculated to explore the potential of dysregulated enzymes and pathways.

RNA isolation and real-time quantitative polymerase chain reaction (PCR) analysis

Total RNA was isolated from the extracted serum exosomes. First-strand complementary DNA (cDNA) was generated from normalized RNA using random hexamer primers and the Superscript II kit (Invitrogen). Primers were designed by the Roche Universal Probe Library Assay Design Center. Two units of sensiFAST probe No-ROX Mix (Bioline) were used in each 96-well reaction plate (Axon). A Roche LightCycler® 480 was used to perform the quantitative polymerase chain reaction (qPCR) and the real-time qPCR was repeated three times for each condition (25).

Statistical analysis

Data are presented as mean ± standard error of the mean (SEM). for continuous variables and as a percentage for categorical variables. The miRNA reads were mapped to the miRBase human miRNA reference database using the FANSe3 algorithm and data were processed on the Chi-Cloud NGS Analysis Platform as described in previous publications (21). The expression levels of miRNAs in liver blood, lung blood, and peripheral blood were extracted from the Human miRNA Tissue Atlas (26). The serum metabolomics data were normalized using

© Annals of Translational Medicine. All rights reserved.

Table 1 Clinical characteristics of the patients with CAP or VAP caused by Ab Infection

Characteristics	VAP with Ab	CAP	P
Age (years)	60.33±10.12	67.20±6.30	ns
Female	0.33%	0.40%	
WBC ($\times10^9$/L)	10.88±1.85	11.75±7.32	ns
Neutrophil% (%)	90.57±5.13	84.70±13.09	ns
CRP (mg/L)	78.33±26.04	103.98±107.85	ns
PCT (μg/L)	2.40±3.85	0.45±0.61	ns

Ab, *Acinetobacter baumannii*; CAP, community-acquired pneumonia; CRP, C-reactive protein; PCT, procalcitonin; WBC, white blood cell; VAP, ventilator-associated pneumonia.

MetaboAnalyst before they were analyzed as described in previous publications (27-36). Enrichment analyses were performed based on metabolic pathway-associated and drug pathway-associated metabolite sets (37,38). Correlation and regression analyses of metabolites with the demographic information and biochemical measurements were calculated using Pearson's correlation (SPSS 20.0). Heatmaps and volcano plots were created using R studio. P values of <0.05 were considered statistically significant.

Results

BALF exosomes and serum exosomes indicated differential miRNA profiles in Ab-VAP patients compared with CAP patients

To explore whether exosomal miRNA profiles were altered in Ab-VAP patients, we collected BALF from these patients and from control CAP patients (*Table 1*), and performed exosome isolation using SBI kits (*Figure 1A*). Exosome sizes were measured by electron microscopy (*Figure 1B*), and we also sequenced the exosomal miRNAs. We found that miRNAs were differentially modulated in Ab-VAP patients compared with control patients. This is shown in a heatmap of the top 198 altered miRNAs (*Figure 1C*) and a volcano plot (*Figure 1D*). The top 25 downregulated miRNAs are shown in *Figure 1E* and the top 25 upregulated miRNAs are shown in *Figure 1F*. To determine if these differential miRNAs were derived from lung tissue, we searched the Human miRNA Tissue Atlas (26), as shown in *Table 2*. We found that, in general, these miRNAs were highly expressed in lung tissue. This further suggests that the exosomes came from lung tissue.

Significantly altered miRNA expression in BALF was correlated with serum exosome expression

A recent study identified the systemic function of exosomal miRNAs that target gene expression in liver metabolism (7). We therefore searched the Human miRNA Tissue Atlas to determine if the top 25 miRNAs with altered profiles (26), as found in our study, were expressed in liver blood and peripheral blood. The expression levels of the top 25 differentially expressed miRNAs in liver blood, lung blood, and peripheral blood are listed in Table S2. We selected miRNAs from the Human miRNA Tissue Atlas that are expressed more abundantly in the serum exosome In line with the results of our BALF analysis, qPCR analysis of serum exosomes also showed significant differential expression of miRNAs such as miR-338-3p, miR-26b-5p, miR-30e-5p, and miR-424-5p (*Figure 2A*). This suggests that miRNAs excreted from lung cells can enter the circulatory system and affect distant organs.

Differentially expressed miRNAs were significantly enriched in metabolic pathways

As differentially expressed miRNAs were detected in Ab-VAP patients, we sought to determine if these altered miRNA profiles played a crucial role in metabolic pathways. We used KEGG pathway analysis and Gene Ontology enrichment analysis based on the top 100 differential miRNAs found in our study. KEGG pathway analysis showed enrichment of a number of molecules related to metabolic signaling pathways, including PI3K-Akt, thyroid hormone, and AMPK; these molecules were also enriched in other cancer-related and cytoskeleton signaling pathways

© Annals of Translational Medicine. All rights reserved.

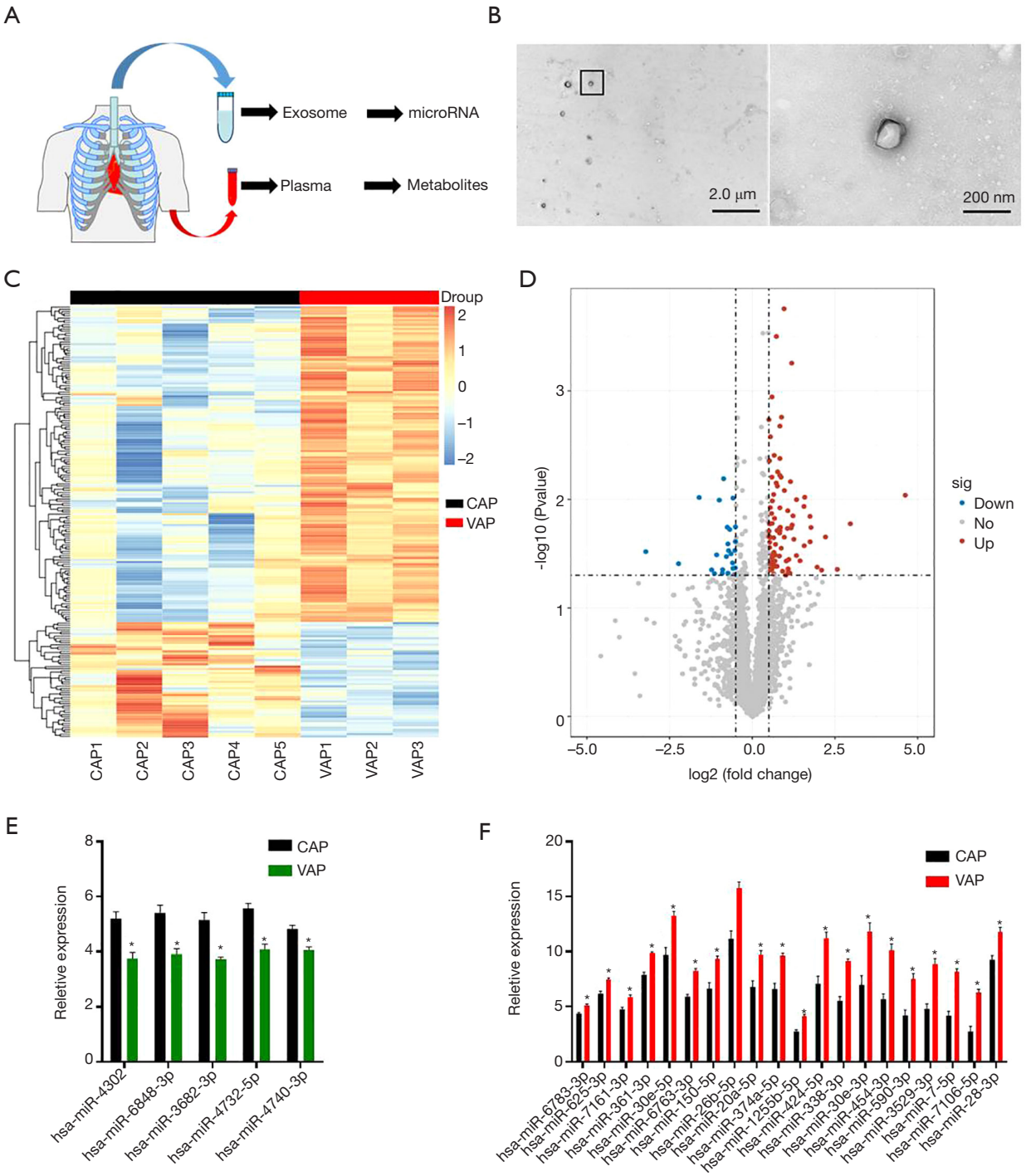

Figure 1 BALF exosomes and serum exosomes indicated differential miRNA profiles in Ab-VAP patients compared with CAP patients. (A) Study protocol for the isolation of EVs in bronchoalveolar lavage fluid and serum sample collection. (B) Characterization of bronchoalveolar exosomes using electron microscopy. Scale bar: 2.0 μm and 200 nm respectively. (C) Heatmap showing 198 microRNAs altered in 3 VAP patients caused by Ab and 5 CAP patients. (D) Volcano plot of the dysregulated microRNAs. Red dots indicated upregulated microRNAs with P<0.05 and Fold Change >2 with upregulation. Blue dots indicated downregulated microRNAs with P<0.05 and Fold Change >2 with down regulation. Grey dots indicated microRNAs with P>0.05 or Fold Change <2. (E) Alteration of down regulated microRNAs in VAP as compared to CAP. (F) Alteration of up regulated microRNAs in VAP as compared to CAP. *, P<0.05.

© Annals of Translational Medicine. All rights reserved.

Table 2 List of the top 25 differentially expressed microRNA and their expression in liver, long and normal blood

miRNA	log_2_FC (VAP/CAP)	P value	FDR	Lung	Liver	Blood
Down regulated miRNAs						
hsa-miR-4732-5p	−0.45	0.00	0.50	120.98	77.68	–
hsa-miR-6848-3p	−0.47	0.00	0.57	–	–	–
hsa-miR-3682-3p	−0.47	0.00	0.57	94.84	84.62	2.06
hsa-miR-4740-3p	−0.25	0.00	0.57	6.31	16.01	–
hsa-miR-4302	−0.47	0.00	0.57	–	–	–
Up regulated miRNAs						
hsa-miR-361-3p	0.32	0.00	0.20	42.77	22.93	7.60
hsa-miR-6763-3p	0.48	0.00	0.20	–	–	–
hsa-miR-338-3p	0.73	0.00	0.20	978.49	8.10	2.50
hsa-miR-7-5p	0.96	0.00	0.20	17.88	5.81	4.33
hsa-miR-7106-5p	1.19	0.00	0.28	12.44	2.68	2.29
hsa-miR-1255b-5p	0.59	0.00	0.48	12.44	2.67	2.29
hsa-miR-625-3p	0.27	0.00	0.50	22.42	26.02	2.54
hsa-miR-26b-5p	0.50	0.00	0.50	282.91	78.18	6.60
hsa-miR-454-3p	0.83	0.00	0.50	11.07	4.70	3.20
hsa-miR-3529-3p	0.88	0.00	0.50	–	–	–
hsa-miR-374a-5p	0.55	0.00	0.56	47.48	23.35	4.24
hsa-miR-6783-3p	0.23	0.00	0.57	–	–	–
hsa-miR-30e-5p	0.45	0.00	0.57	364.54	478.85	6.12
hsa-miR-150-5p	0.49	0.00	0.57	83.49	12.56	12.19
hsa-miR-20a-5p	0.52	0.00	0.57	197.03	114.56	7.75
hsa-miR-424-5p	0.66	0.00	0.57	111.30	92.46	2.80
hsa-miR-590-5p	0.83	0.00	0.57	31.09	10.52	2.44
hsa-miR-7161-3p	0.30	0.01	0.57	–	–	–
hsa-miR-30e-3p	0.76	0.01	0.57	59.57	12.38	4.15
hsa-miR-28-3p	0.35	0.01	0.57	12.18	10.12	1.64

–, not found in human miRNA tissue atlas.

(*Figure 3A*; Table S1). Gene Ontology enrichment analysis further showed enrichment in metabolism and cell–cell crosstalk, as demonstrated by biological processes, cellular components, and molecular functions (*Figure 3B*; Table S2).

Serum metabolites were differentially regulated in Ab-VAP patients

Alterations in miRNA expression profiles and the results of our enrichment analysis indicated that BALF exosomal miRNA may play a role in systemic metabolism. We therefore investigated changes in the circulatory metabolic profiles of Ab-VAP patients. A total of 227 serum metabolites, including alcohols, amino acids, carbohydrates, and fatty acids, were detected in the serum of these patients. The differences in overall metabolite class values between the Ab-VAP patients and the control CAP patients are presented as a heatmap. No significant differences existed

© Annals of Translational Medicine. All rights reserved.

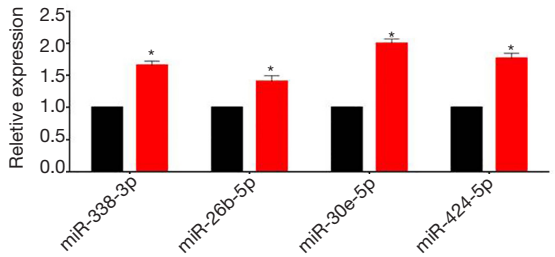

Figure 2 Significantly altered miRNA expression in BALF was correlated with serum exosome expression. (A) Relative expression of microRNAs in VAP as compared to CAP in the serum exosomes. *, P<0.05.

between the two groups (*Figure 4A*).

We then compared the metabolite levels and ratios of biological significance between CAP patients and Ab-VAP patients. A volcano plot was used to show significantly altered metabolite profiles and ratios with P values of <0.05 with fold change more than twice (*Figure 4B*). Of these metabolites, the profiles of hydroxypropionic acid, D-Xylose, ornithine, and caproic acid (*Figure 4C*) were found to be significantly altered. The ratios of biological significance between L-valine and alpha-Ketoisovaleric acid, as well as that between tryptamine and L-tryptophan (*Figure 4D*), were also significantly altered.

Serum metabolites were differentially regulated in metabolic pathway-associated metabolite sets and drug pathway-associated metabolite sets in Ab-VAP patients

Based on the circulatory metabolic profiles described above, we further determined whether this altered metabolite expression played a role in different metabolic pathways. Enrichment analyses were performed to identify metabolite sets grouped by involvement with the same biological processes or drug-associated pathways. The strongest associations between altered metabolite expression and different biological processes were found in the urea cycle and phenylacetate metabolism (*Figure 5A*; Table S3). As Ab infections have a long duration and are resistant to antibiotics, we also analyzed the relationships between altered metabolite profiles and drug-associated pathways in the two groups. Metabolites with altered expression in Ab-VAP patients were shown to be involved in a number of drug pathways (*Figure 5B*; Table S4). These pathways are associated with cell cycle suppression through the inhibition of purine metabolism.

Differential BALF exosomal miRNAs were correlated with serum metabolite levels

As we found alterations in both BALF exosomal miRNA profiles and serum metabolite profiles in Ab-VAP patients, we then investigated the relationship between BALF miRNA and systemic metabolism. First, we analyzed the correlations between the top 25 altered BALF exosomal miRNA profiles and classes of metabolites. All 25 miRNAs were significantly correlated with serum alcohol levels, and a majority of these miRNAs were also significantly correlated with indoles; this is consistent with the alterations found in the metabolite ratios (*Figure 6A*). *Figure 6B* shows lines drawn to connect metabolites and miRNAs with significant correlations in a network. These correlation analyses also confirmed that hydroxypropionic acid and ornithine were significantly correlated with several miRNAs, which indicates pathophysiological significance (Table S5). We can infer from this and our results that exosomes released from lung immune and structural cells may enter the circulatory system and carry miRNAs to the liver. Once in the liver, these miRNAs perform functions that affect serum metabolite profiles (*Figure 6C*). The exact mechanism by which these miRNAs achieve this, however, requires *in vivo* and *in vitro* investigation.

Discussion

Although BALF exosomal miRNAs have been shown to regulate a wide range of inflammatory processes (4,8-11), their function in patients with Ab infection has yet to be investigated. In the present study, we found significantly altered exosomal miRNA profiles in the BALF of patients with Ab-VAP. Gene Ontology analysis further distinguished the functions of these miRNAs in systemic metabolism. We also found that the serum metabolomic profiles and ratios of biological significance were differentially regulated in patients with Ab-VAP; these changes were correlated with the differential expression of miRNAs. The differential expression pattern of exosomal miRNAs found in the lungs, liver, and circulation implies that BALF exosomes originating from immune and structural lung cells might carry miRNAs into the circulatory system to target systemic metabolism.

Although BALF has been shown to be involved in the development of asthma, lung cancer, and interstitial lung disease (4,8-11), its role in pulmonary infections remains unclear. Respiratory exosomes, nanovesicles circulating in

© Annals of Translational Medicine. All rights reserved.

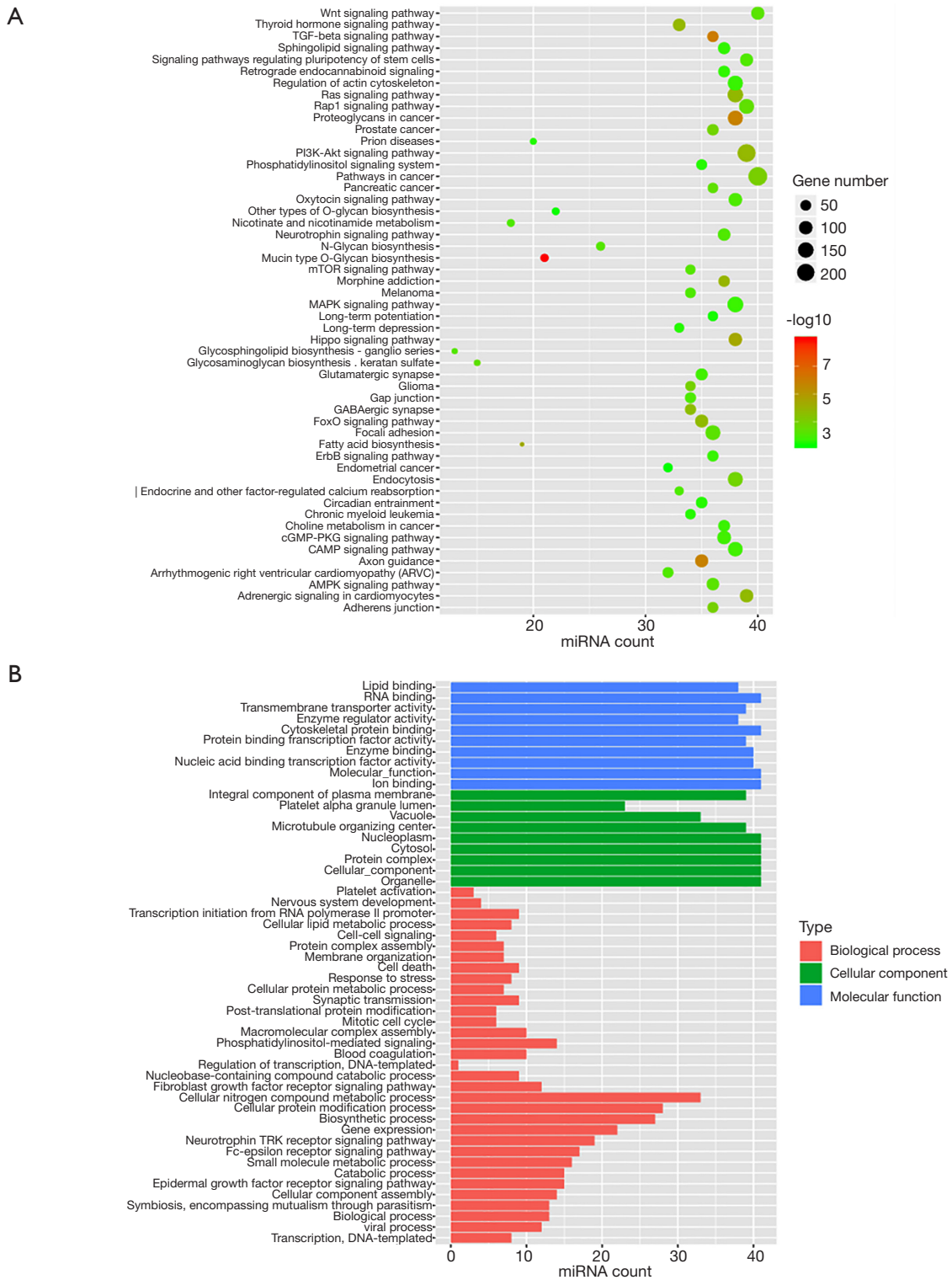

Figure 3 Differentially expressed miRNAs were significantly enriched in metabolic pathways. (A) The KEGG pathway analysis based on top 100 differential miRNAs identified significant enrichment in a number of metabolism related signaling, including PI3K-Akt, thyroid hormone, AMPK, etc. (B) The Gene Ontology enrichment analysis based on top 100 differential miRNAs revealed enrichment in metabolism and cell-cell crosstalk as displayed by biological process, cellular component and molecular function.

© Annals of Translational Medicine. All rights reserved.

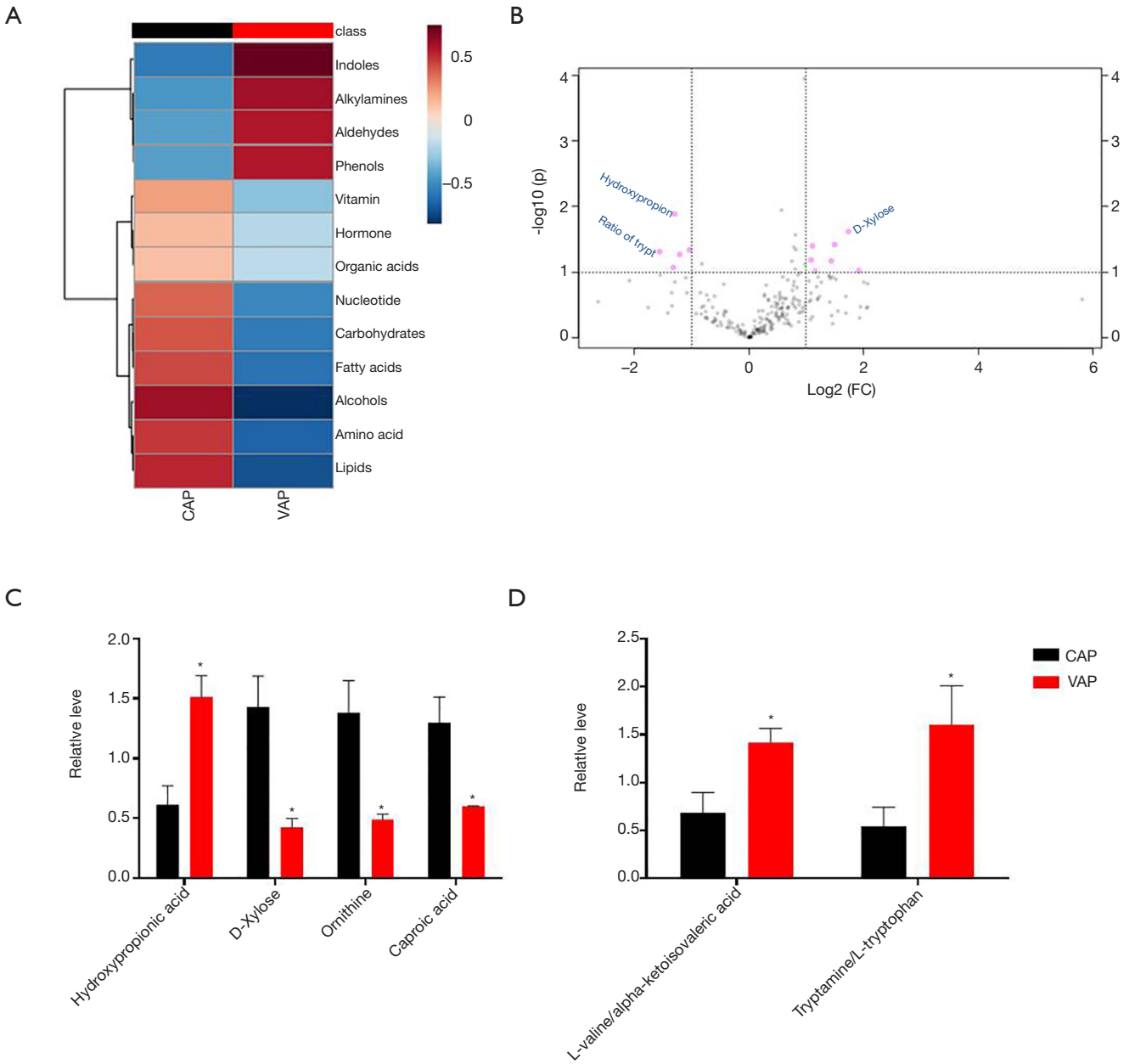

Figure 4 Serum metabolites were differentially regulated in Ab-VAP patients. (A) Heatmap showing metabolites classes between CAP and VAP with Ab infection. (B) Volcano plot of the dysregulated metabolites and ratios of biological significance. Red dots indicated upregulated metabolites with P<0.05 and Fold Change >2. Blue dots indicated downregulated metabolites with P<0.05 and Fold Change >2. Grey dots indicated microRNAs alteration with P>0.05 or Fold Change <2. (C) Relative levels of significantly altered metabolites in VAP caused by Ab infection as compared to CAP. (D) Relative levels of significantly altered ratios of biological significance in VAP caused by Ab infection as compared to CAP. Data were analyzed using Student *t*-test. mean ± SE. *, P<0.05.

© Annals of Translational Medicine. All rights reserved.

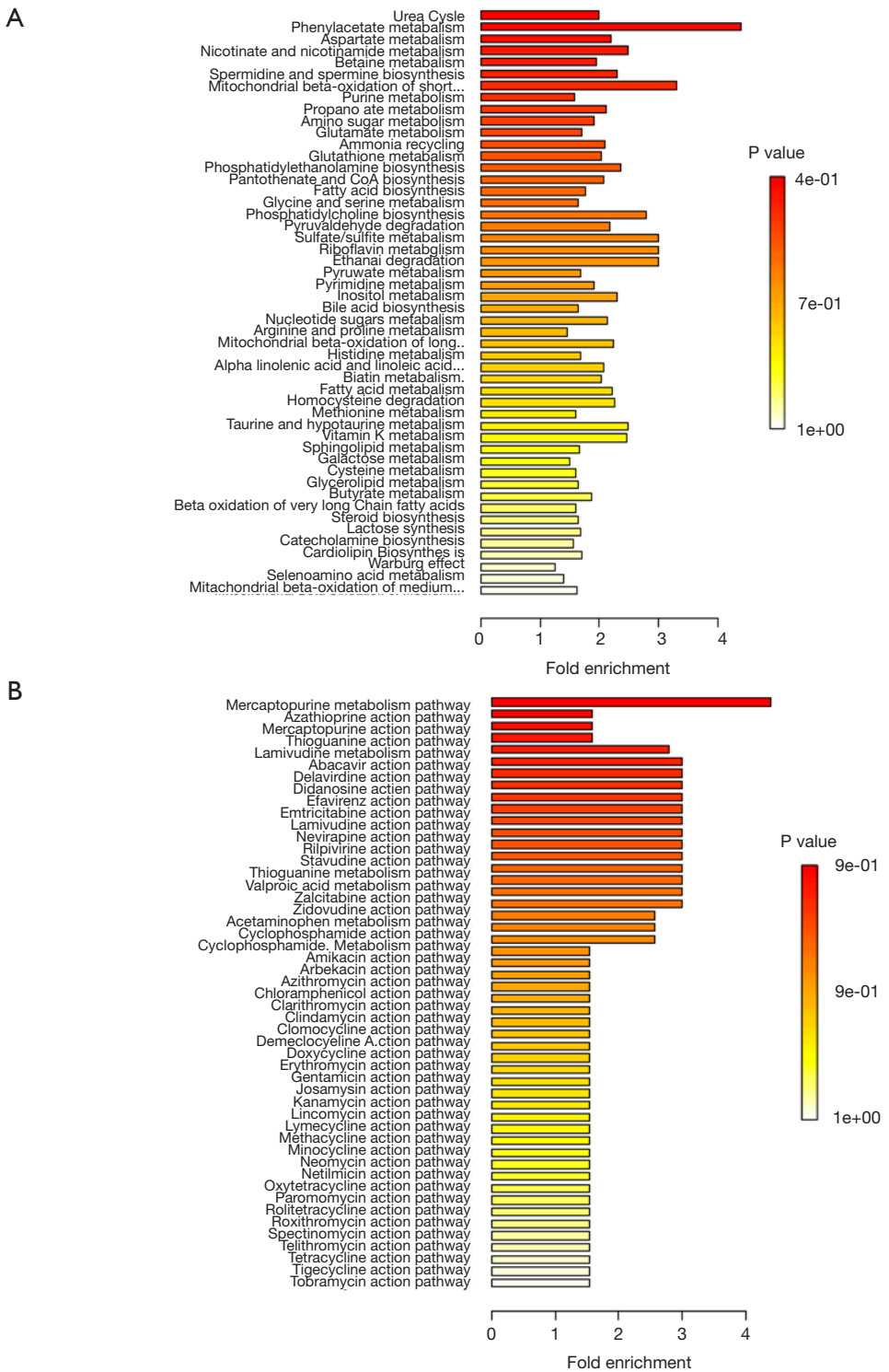

Figure 5 Serum metabolites were differentially regulated in metabolic pathway-associated metabolite sets and drug pathway-associated metabolite sets in Ab-VAP patients. (A) Enrichment analysis of metabolites based on pathway-associated metabolite sets. The strongest association was found in Urea Cycle and Phenylacetate Metabolism. (B) Enrichment analysis of metabolites based on drug-pathway-associated metabolite sets, pointing to altered drug pathways correlating to suppressing cell cycle by inhibiting purine metabolism.

© Annals of Translational Medicine. All rights reserved.

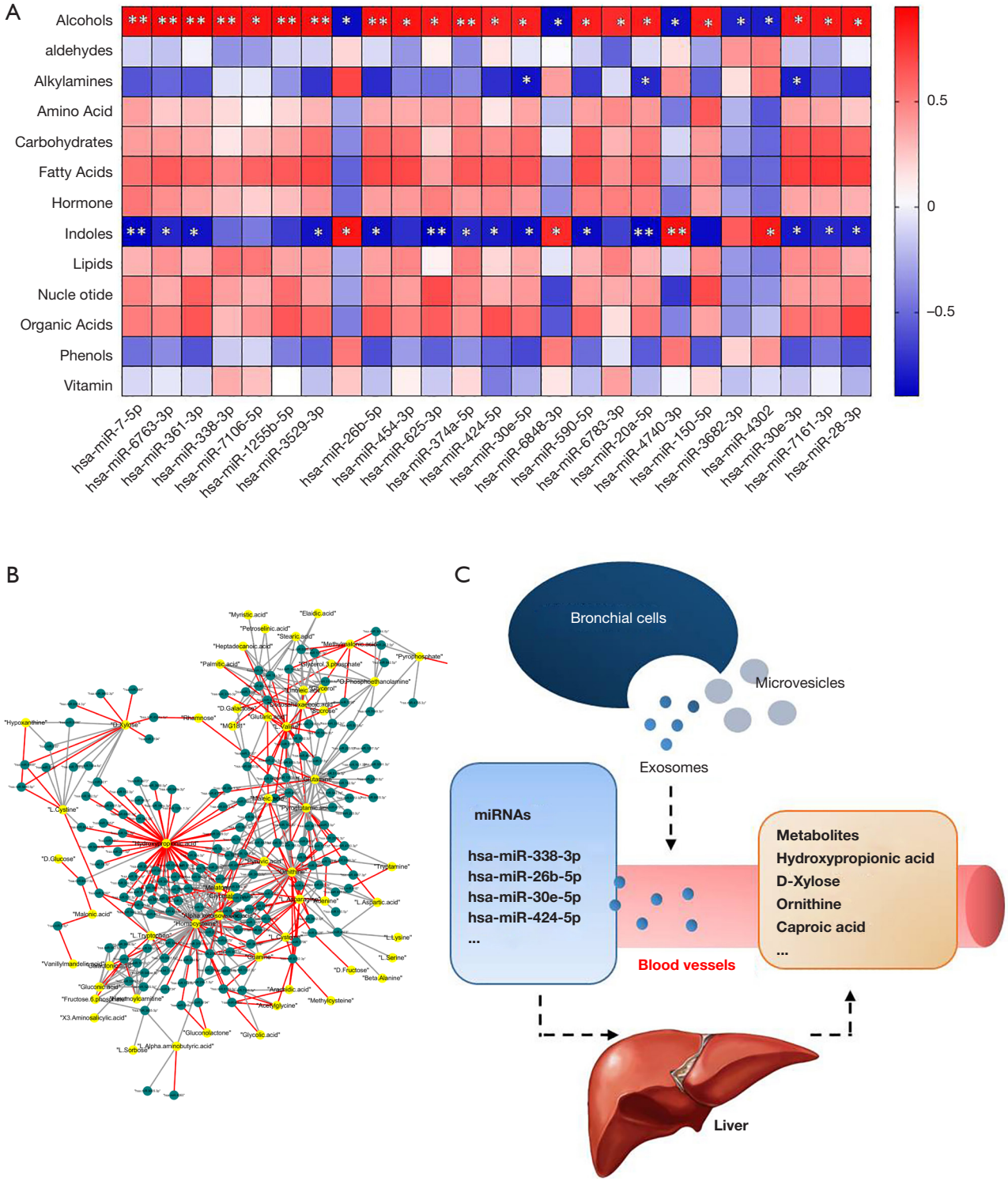

Figure 6 Differential BALF exosomal miRNAs were correlated with serum metabolite levels. (A) Correlations between BALF exosome microRNAs and serum metabolites levels. The colors in the heatmap stood for efficiency of the Pearson's correlation. *, P<0.05, **, P<0.01. (B) Correlated metabolites and microRNAs identified and connected with lines in the network. (C) Schematic illustration that exosomes released from the lung tissue might enter circulation, carry microRNAs from both immune and structural cells to the liver and exert subsequent effects to serum metabolite profile.

© Annals of Translational Medicine. All rights reserved.

the respiratory tract, have been shown to be involved in the progression of inflammation-related lung damage (6). The present study examined the miRNA content of lung-derived exosomes isolated from BALF in Ab-VAP patients and CAP patients. The differential regulation of exosomal miRNAs that occurs in VAP suggests that lung-derived exosomes are involved in the propagation of this disease during Ab infection. The discovery of these alterations of BALF exosomal miRNA profiles provides potential biomarkers and novel insight into the underlying mechanisms of Ab infection, as well as the development of strategies to treat this infection.

Studies on serum metabolism have provided evidence that improves the understanding of pathophysiological mechanisms of pulmonary infectious diseases. These studies have shown that many serum metabolites could be used as biomarkers to detect metabolic disorders in patients with pneumonia (13,14). Although metabolic disturbances are known to occur in pneumonia, few studies have discussed metabolic profile changes in pneumonia patients infected with Ab. Our results have shown that serum metabolism is differentially regulated during Ab infection. It should be noted that, in our study, only a few serum metabolites showed altered profiles in VAP patients compared with CAP patients. One reason for this could be our limited sample size. Another could be that, since both CAP and VAP are associated with systemic inflammation, circulatory metabolites might have undergone similar inflammatory changes. Whatever the cause, these metabolites that are differentially expressed in Ab-VAP have been shown to affect several drug pathways involved in the suppression of cell cycles by purine metabolism inhibition. This identifies several potential therapeutic targets for this disease, although their pathophysiological mechanisms require further exploration.

The primary novelty of our results is the notion that exosomal miRNAs derived from the lungs might enter blood circulation and regulate systemic metabolism. Consistent with these findings, we found that differentially expressed miRNAs carried in BALF exosomes are present in blood samples taken from the lungs, liver, and peripheral blood. We also found that these altered miRNA levels are correlated with changes in circulatory metabolism. This implies that BALF exosomes derived from both immune and structural lung cells might carry miRNAs into the circulatory system. Once in this system, the miRNAs are transported to target metabolism-related organs where they carry out functions that regulate the circulatory metabolism profile.

The primary limitation of the present study was that the sample size was relatively small; few patients between the ages of 50 and 75 with critical pulmonary infections met our study's inclusion criteria. Finding and recruiting CAP and VAP patients admitted to the ICU due to pulmonary infection who also have no notable medical history, including severe renal or hepatic damage, is challenging. Additionally, although we can infer from our results that lung tissue-derived exosomes might be released into peripheral blood circulation and modulate metabolism in Ab-VAP patients, further *in vitro* and *in vivo* studies are necessary to confirm both this cell-cell crosstalk function and the organs targeted by BALF exosomes.

Conclusions

The present study identified altered BALF exosomal miRNA profiles in Ab-VAP patients. These miRNAs are enriched in metabolism-related pathways and are correlated with serum metabolism changes during Ab infection. Our data implies that lung-derived exosomal miRNAs might enter the peripheral blood circulation and regulate systemic metabolism. These metabolic changes could indicate potential novel metabolic targets for the treatment of Ab infection.

Acknowledgments

We thank all patients involved in the study.
Funding: This study was supported by National Natural Science Foundation of China (81800390), Key Research and Development Program of Shaanxi (Program No. 2020KW-049)x, the Fundamental Research Funds for the Central Universities in China (1191329724, 191329849), and the Clinical Research Award of the First Affiliated Hospital of Xi'an Jiaotong University in China (XJTU1AF-CRF-2018-025).

Footnote

Data Sharing Statement: Available at http://dx.doi.org/10.21037/atm-20-2375

Conflicts of Interest: All authors have completed the ICMJE uniform disclosure form (available at http://dx.doi.org/10.21037/atm-20-2375). The authors have no conflicts of interest to declare.

© Annals of Translational Medicine. All rights reserved.

Ethical Statement: The authors are accountable for all aspects of the work in ensuring that questions related to the accuracy or integrity of any part of the work are appropriately investigated and resolved. Written informed consent was obtained according to the Declaration of Helsinki (as revised in 2013), and was approved by the ethics committee, Xi'an Jiaotong University (2018G-169).

Open Access Statement: This is an Open Access article distributed in accordance with the Creative Commons Attribution-NonCommercial-NoDerivs 4.0 International License (CC BY-NC-ND 4.0), which permits the non-commercial replication and distribution of the article with the strict proviso that no changes or edits are made and the original work is properly cited (including links to both the formal publication through the relevant DOI and the license). See: https://creativecommons.org/licenses/by-nc-nd/4.0/.

References

1. Nair GB, Niederman MS. Ventilator-associated pneumonia: present understanding and ongoing debates. Intensive Care Med 2015;41:34-48.
2. Zilberberg MD, Nathanson BH, Sulham K, et al. A Novel Algorithm to Analyze Epidemiology and Outcomes of Carbapenem Resistance Among Patients With Hospital-Acquired and Ventilator-Associated Pneumonia: A Retrospective Cohort Study. Chest 2019;155:1119-30.
3. Huang Y, Zhou Q, Wang W, et al. Acinetobacter baumannii Ventilator-Associated Pneumonia: Clinical Efficacy of Combined Antimicrobial Therapy and in vitro Drug Sensitivity Test Results. Front Pharmacol 2019;10:92.
4. Yang Y, Ji P, Wang X, et al. Bronchoalveolar Lavage Fluid-Derived Exosomes: A Novel Role Contributing to Lung Cancer Growth. Front Oncol 2019;9:197.
5. Lee H, Groot M, Pinilla-Vera M, et al. Identification of miRNA-rich vesicles in bronchoalveolar lavage fluid: Insights into the function and heterogeneity of extracellular vesicles. J Control Release 2019;294:43-52.
6. Rollet-Cohen V, Bourderioux M, Lipecka J, et al. Comparative proteomics of respiratory exosomes in cystic fibrosis, primary ciliary dyskinesia and asthma. J Proteomics 2018;185:1-7.
7. Thomou T, Mori MA, Dreyfuss JM, et al. Adipose-derived circulating miRNAs regulate gene expression in other tissues. Nature 2017;542:450-5.
8. Moon HG, Cao Y, Yang J, et al. Lung epithelial cell-derived extracellular vesicles activate macrophage-mediated inflammatory responses via ROCK1 pathway. Cell Death Dis 2015;6:e2016.
9. Maemura T, Fukuyama S, Sugita Y, et al. Lung-Derived Exosomal miR-483-3p Regulates the Innate Immune Response to Influenza Virus Infection. J Infect Dis 2018;217:1372-82.
10. Qiao Y, Liang X, Yan Y, et al. Identification of Exosomal miRNAs in Rats With Pulmonary Neutrophilic Inflammation Induced by Zinc Oxide Nanoparticles. Front Physiol 2018;9:217.
11. Levanen B, Bhakta NR, Torregrosa Paredes P, et al. Altered microRNA profiles in bronchoalveolar lavage fluid exosomes in asthmatic patients. J Allergy Clin Immunol 2013;131:894-903.
12. Chen J, Hu C, Pan P. Extracellular Vesicle MicroRNA Transfer in Lung Diseases. Front Physiol 2017;8:1028.
13. Chiu CY, Lin G, Cheng ML, et al. Metabolomic Profiling of Infectious Parapneumonic Effusions Reveals Biomarkers for Guiding Management of Children with Streptococcus pneumoniae Pneumonia. Sci Rep 2016;6:24930.
14. Seymour CW, Yende S, Scott MJ, et al. Metabolomics in pneumonia and sepsis: an analysis of the GenIMS cohort study. Intensive Care Med 2013;39:1423-34.
15. Brown RL, Sequeira RP, Clarke TB. The microbiota protects against respiratory infection via GM-CSF signaling. Nat Commun 2017;8:1512.
16. McFarlane AJ, McSorley HJ, Davidson DJ, et al. Enteric helminth-induced type I interferon signaling protects against pulmonary virus infection through interaction with the microbiota. J Allergy Clin Immunol 2017;140:1068-78.e6.
17. Brown RL, Clarke TB. The regulation of host defences to infection by the microbiota. Immunology 2017;150:1-6.
18. She J, Guo M, Li H, et al. Targeting amino acids metabolic profile to identify novel metabolic characteristics in atrial fibrillation. Clin Sci (Lond) 2018;132:2135-46.
19. She J, Feng J, Deng Y, et al. Correlation of Triiodothyronine Level with In-Hospital Cardiac Function and Long-Term Prognosis in Patients with Acute Myocardial Infarction. Dis Markers 2018;2018:5236267.
20. She J, Deng Y, Wu Y, et al. Hemoglobin A1c is associated with severity of coronary artery stenosis but not with long term clinical outcomes in diabetic and nondiabetic patients with acute myocardial infarction undergoing primary angioplasty. Cardiovasc Diabetol 2017;16:97.
21. Liu W, Xiang L, Zheng T, et al. TranslatomeDB: a comprehensive database and cloud-based analysis platform

© Annals of Translational Medicine. All rights reserved.

for translatome sequencing data. Nucleic Acids Res 2018;46:D206-D12.
22. Qiu Y, Cai G, Su M, et al. Serum metabolite profiling of human colorectal cancer using GC-TOFMS and UPLC-QTOFMS. J Proteome Res 2009;8:4844-50.
23. Wang JH, Chen WL, Li JM, et al. Prognostic significance of 2-hydroxyglutarate levels in acute myeloid leukemia in China. Proc Natl Acad Sci U S A 2013;110:17017-22.
24. Ni Y, Qiu Y, Jiang W, et al. ADAP-GC 2.0: deconvolution of coeluting metabolites from GC/TOF-MS data for metabolomics studies. Anal Chem 2012;84:6619-29.
25. Sharma KR, Heckler K, Stoll SJ, et al. ELMO1 protects renal structure and ultrafiltration in kidney development and under diabetic conditions. Sci Rep 2016;6:37172.
26. Ludwig N, Leidinger P, Becker K, et al. Distribution of miRNA expression across human tissues. Nucleic Acids Res 2016;44:3865-77.
27. Xia J, Wishart DS. Using MetaboAnalyst 3.0 for Comprehensive Metabolomics Data Analysis. Curr Protoc Bioinformatics 2016;55:14.10.1-14.10.91.
28. Xia J, Sinelnikov IV, Han B, et al. MetaboAnalyst 3.0--making metabolomics more meaningful. Nucleic Acids Res 2015;43:W251-7.
29. Xia J, Mandal R, Sinelnikov IV, et al. MetaboAnalyst 2.0--a comprehensive server for metabolomic data analysis. Nucleic Acids Res 2012;40:W127-33.
30. Xia J, Wishart DS. Web-based inference of biological patterns, functions and pathways from metabolomic data using MetaboAnalyst. Nat Protoc 2011;6:743-60.
31. Xia J, Wishart DS. Metabolomic data processing, analysis, and interpretation using MetaboAnalyst. Curr Protoc Bioinformatics 2011;Chapter 14:Unit 14 0.
32. Xia J, Psychogios N, Young N, et al. MetaboAnalyst: a web server for metabolomic data analysis and interpretation. Nucleic Acids Res 2009;37:W652-60.
33. Xia J, Broadhurst DI, Wilson M, et al. Translational biomarker discovery in clinical metabolomics: an introductory tutorial. Metabolomics 2013;9:280-99.
34. Xia J, Sinelnikov IV, Wishart DS. MetATT: a web-based metabolomics tool for analyzing time-series and two-factor datasets. Bioinformatics 2011;27:2455-6.
35. Xia J, Wishart DS. MetPA: a web-based metabolomics tool for pathway analysis and visualization. Bioinformatics 2010;26:2342-4.
36. Xia J, Wishart DS. MSEA: a web-based tool to identify biologically meaningful patterns in quantitative metabolomic data. Nucleic Acids Res 2010;38:W71-7.
37. Frolkis A, Knox C, Lim E, et al. SMPDB: The Small Molecule Pathway Database. Nucleic Acids Res 2010;38:D480-7.
38. Jewison T, Su Y, Disfany FM, et al. SMPDB 2.0: big improvements to the Small Molecule Pathway Database. Nucleic Acids Res 2014;42:D478-84.

Cite this article as: Zhou B, Guo M, Hao X, Lou B, Liu J, She J. Altered exosomal microRNA profiles in bronchoalveolar lavage fluid can mediate metabolism in patients with *Acinetobacter baumannii* ventilator-associated pneumonia. Ann Transl Med 2020;8(23):1561. doi: 10.21037/atm-20-2375

© Annals of Translational Medicine. All rights reserved.

Supplementary

Table S1 KEGG enrichment analysis of the differentially expressed microRNAs

KEGG pathway	P value	#Genes	#miRNAs
Mucin type O-Glycan biosynthesis	1.16E-09	23	21
TGF-beta signaling pathway	0.000000939	60	36
Axon guidance	0.00000153	94	35
Proteoglycans in cancer	0.00000153	136	38
Hippo signaling pathway	0.0000364	101	38
Fatty acid biosynthesis	0.0000535	7	19
Morphine addiction	0.000112304	63	37
Thyroid hormone signaling pathway	0.000139178	84	33
PI3K-Akt signaling pathway	0.000139178	224	39
Ras signaling pathway	0.000157576	151	38
FoxO signaling pathway	0.000169242	93	35
Adrenergic signaling in cardiomyocytes	0.000180077	101	39
GABAergic synapse	0.00023194	58	34
Pathways in cancer	0.000911844	246	40
Adherens junction	0.001096546	55	36
Glioma	0.001104613	46	34
Endocytosis	0.001402455	134	38
Prostate cancer	0.001449483	64	36
Glycosaminoglycan biosynthesis - keratan sulfate	0.003845853	12	15
Rap1 signaling pathway	0.003845853	136	39
Pancreatic cancer	0.003939949	49	36
Focal adhesion	0.004893039	135	36
AMPK signaling pathway	0.005127382	83	36
Wnt signaling pathway	0.005198956	95	40
Glycosphingolipid biosynthesis - ganglio series	0.006251308	10	13
mTOR signaling pathway	0.006251308	44	34
N-Glycan biosynthesis	0.00636058	31	26
Melanoma	0.008399668	51	34
Nicotinate and nicotinamide metabolism	0.008549548	20	18
Arrhythmogenic right ventricular cardiomyopathy (ARVC)	0.008549548	54	32
Neurotrophin signaling pathway	0.008549548	83	37
Signaling pathways regulating pluripotency of stem cells	0.008549548	91	39
Oxytocin signaling pathway	0.009078433	102	38
Endocrine and other factor-regulated calcium reabsorption	0.009219605	31	33
Gap junction	0.009219605	57	34
Glutamatergic synapse	0.01470712	74	35
cGMP-PKG signaling pathway	0.01486864	107	37
cAMP signaling pathway	0.015166575	127	38
Choline metabolism in cancer	0.018244195	69	37
MAPK signaling pathway	0.019036457	160	38
ErbB signaling pathway	0.019442331	59	36
Regulation of actin cytoskeleton	0.019577433	137	38
Sphingolipid signaling pathway	0.023605903	76	37
Retrograde endocannabinoid signaling	0.02462814	68	37
Long-term depression	0.031399414	40	33
Chronic myeloid leukemia	0.031399414	48	34
Phosphatidylinositol signaling system	0.031399414	53	35
Circadian entrainment	0.031399414	64	35
Prion diseases	0.032819541	13	20
Long-term potentiation	0.041227469	46	36
Other types of O-glycan biosynthesis	0.045799651	19	22
Endometrial cancer	0.049107072	35	32

© Annals of Translational Medicine. All rights reserved.
http://dx.doi.org/10.21037/atm-20-2375

Table S2 GO enrichment analysis of the differentially expressed microRNAs

GO_Category	P value	genes	miRNAs	CAT
Transcription, DNA-templated	0	794	8	BP
Viral process	0	221	12	BP
Biological_process	0	6,124	13	BP
Symbiosis, encompassing mutualism through parasitism	0	255	13	BP
Cellular component assembly	0	568	14	BP
Epidermal growth factor receptor signaling pathway	0	121	15	BP
Catabolic process	0	904	15	BP
Small molecule metabolic process	0	1062	16	BP
Fc-epsilon receptor signaling pathway	0	105	17	BP
Neurotrophin TRK receptor signaling pathway	0	170	19	BP
Gene expression	0	343	22	BP
Biosynthetic process	0	2,113	27	BP
Cellular protein modification process	0	1,234	28	BP
Cellular nitrogen compound metabolic process	0	2,664	33	BP
Fibroblast growth factor receptor signaling pathway	4.44E-15	95	12	BP
Nucleobase-containing compound catabolic process	2.76E-14	385	9	BP
Regulation of transcription, DNA-templated	7.34E-13	157	1	BP
Blood coagulation	9.06E-13	197	10	BP
Phosphatidylinositol-mediated signaling	9.54E-13	75	14	BP
Macromolecular complex assembly	3.31E-12	337	10	BP
Mitotic cell cycle	1.04E-09	141	6	BP
Post-translational protein modification	1.11E-09	70	6	BP
Synaptic transmission	1.60E-09	182	9	BP
Cellular protein metabolic process	2.07E-09	159	7	BP
Response to stress	1.10E-08	701	8	BP
Cell death	1.83E-07	354	9	BP
Membrane organization	9.56E-07	227	7	BP
Protein complex assembly	2.19E-05	229	7	BP
Cell-cell signaling	3.32E-05	206	6	BP
Cellular lipid metabolic process	5.53E-05	63	8	BP
Transcription initiation from RNA polymerase II promoter	0.0001051	89	9	BP
Nervous system development	0.0034436	111	4	BP
Platelet activation	0.0491226	55	3	BP
Organelle	0	5,442	41	CC
Cellular_component	2.92E-43	8,635	41	CC
Protein complex	3.58E-40	1,964	41	CC
Cytosol	7.59E-35	1,445	41	CC
Nucleoplasm	5.25E-27	639	41	CC
Microtubule organizing center	1.57E-09	248	39	CC
Vacuole	0.0033698	148	33	CC
Platelet alpha granule lumen	0.0038401	22	23	CC
Integral component of plasma membrane	0.0221995	574	39	CC
Ion binding	5.02E-207	3,437	41	MF
Molecular_function	1.98E-55	8,591	41	MF
Nucleic acid binding transcription factor activity	4.55E-43	588	40	MF
Enzyme binding	2.25E-37	721	40	MF
Protein binding transcription factor activity	5.47E-28	289	39	MF
Cytoskeletal protein binding	1.82E-19	418	41	MF
Enzyme regulator activity	1.52E-15	433	38	MF
Transmembrane transporter activity	1.98E-07	510	39	MF
RNA binding	0.0001394	846	41	MF
Lipid binding	0.0438036	289	38	MF

© Annals of Translational Medicine. All rights reserved.
http://dx.doi.org/10.21037/atm-20-2375

Table S3 Enrichment analysis of the differentially expressed metabolites based on pathway-associated metabolite sets

Metabolite set	Total	Hits	Statistic	P value	FDR
Urea cycle	29	12	33.33	0.00	0.12
Phenylacetate metabolism	9	2	72.89	0.00	0.12
Aspartate metabolism	35	12	36.73	0.01	0.12
Nicotinate and nicotinamide metabolism	37	4	41.39	0.01	0.12
Betaine metabolism	21	5	32.66	0.01	0.12
Spermidine and spermine biosynthesis	18	5	38.44	0.02	0.29
Mitochondrial beta-oxidation of short chain saturated fatty acids	27	2	55.07	0.03	0.29
Purine metabolism	74	14	26.30	0.03	0.29
Propanoate metabolism	42	8	35.39	0.03	0.29
Amino Sugar metabolism	33	7	31.96	0.04	0.29
Glutamate metabolism	49	13	28.39	0.04	0.29
Ammonia recycling	32	10	35.03	0.05	0.29

Table S4 Enrichment analysis of the differentially expressed metabolites based on drug-pathway-associated metabolite sets

Metabolite set	Total	Hits	Statistic	P value	FDR
Mercaptopurine metabolism pathway	30.00	2.00	72.89	0.00	0.27
Azathioprine action pathway	92.00	14.00	26.30	0.03	0.27
Mercaptopurine action pathway	90.00	14.00	26.30	0.03	0.27
Thioguanine action pathway	91.00	14.00	26.30	0.03	0.27

Table S5 Correlation analysis between serum metabolites and BALF microRNAs

Metabolites	miRNAs	P value	R square
Pyroglutamic.acid	hsa.miR.7.5p	0.004523643	-0.909346748
L.Glutamine	hsa.miR.7.5p	0.003320577	-0.920082013
Ornithine	hsa.miR.7.5p	0.008047844	-0.885241589
L.Glutamine	hsa.miR.6763.3p	0.000162536	-0.976384059
Hydroxypropionic.acid	hsa.miR.6763.3p	0.007987498	0.885595603
Pyroglutamic.acid	hsa.miR.361.3p	0.004970386	-0.905792465
L.Glutamine	hsa.miR.361.3p	0.007688503	-0.887372854
Ornithine	hsa.miR.361.3p	0.003161223	-0.921666119
Glycerol	hsa.miR.338.3p	0.005729458	-0.900157059
L.Glutamine	hsa.miR.338.3p	0.002842403	-0.924982092
Glycerol	hsa.miR.7106.5p	0.003060743	-0.922689137
L.Glutamine	hsa.miR.7106.5p	0.005443204	-0.902228031
Docosahexaenoic.acid	hsa.miR.7106.5p	0.004195379	-0.912091044
L.Valine	hsa.miR.1255b.5p	0.009588036	0.876679564
Pyroglutamic.acid	hsa.miR.1255b.5p	0.003558804	-0.917794733
Ornithine	hsa.miR.1255b.5p	0.006384108	-0.895636677
Docosahexaenoic.acid	hsa.miR.1255b.5p	0.00735205	-0.889421275
Homocysteine	hsa.miR.3529.3p	0.009833993	-0.875387773
L.Glutamine	hsa.miR.3529.3p	0.008270708	-0.883947326
Hydroxypropionic.acid	hsa.miR.3529.3p	0.002536394	0.928376863
L.Glutamine	hsa.miR.4732.5p	0.005494337	0.90185353
Hydroxypropionic.acid	hsa.miR.4732.5p	0.0094514	-0.877405461
Homocysteine	hsa.miR.26b.5p	0.00410986	-0.912826408
Ornithine	hsa.miR.26b.5p	0.009564683	-0.876803205
Hydroxypropionic.acid	hsa.miR.26b.5p	0.002636288	0.927243478
L.Valine	hsa.miR.454.3p	0.007708364	0.887253571
Pyroglutamic.acid	hsa.miR.454.3p	0.001965061	-0.935427835
L.Glutamine	hsa.miR.454.3p	0.008823069	-0.880824015
L.Aspartic.acid	hsa.miR.625.3p	0.007860216	-0.88634739

© Annals of Translational Medicine. All rights reserved.
http://dx.doi.org/10.21037/atm-20-2375